View metadata, citation and similar papers at core.ac.uk

brought to you by CORE

provided by Elsevier - Publisher Connector

Available online at www.sciencedirect.com

ScienceDirect

Energy Procedia 67 (2015) 194 – 202

Energy Procedia

5th Workshop on Metallization for Crystalline Silicon Solar Cells

Failure modes identified during adhesion testing of metal fingers on silicon solar cells

Ran Chen*,Wei Zhang, Xi Wang, Xi Wang, Alison Lennon

School of Photovoltaic and Renewable Energy Engineering, University of New South Wales, Sydney NSW 2052, Australia

Abstract

A stylus-based adhesion tester was used to characterise the adhesion of metal fingers on silicon solar cells. The measured lateral force together with the failure modes of finger cut-off and dislodgment, were identified for screen-printed silver contacts and nickel/copper plated laser-doped selective emitter cells. In-situ images were recorded to visualise the dynamics of the adhesion testing process. The contours of the measured lateral force were mapped to demonstrate the variability of finger adhesion characteristics across two representative solar cells.

© 2015 The Authors. Published by Elsevier Ltd. This is an open access article under the CC BY-NC-ND license (http://creativecommons.org/licenses/by-nc-nd/4.0/).

Peer-review under the responsibility of Gunnar Schubert, Guy Beaucarne and Jaap Hoornstra

Keywords: Adhesion; Metal fingers; Failure modes; Metallisation; Silicon solar cells;

1. Introduction

Strong adhesion of metal contacts to silicon is required for reliable silicon photovoltaic (PV) devices. It is frequently questioned whether plated fingers adhere sufficiently to a silicon surface to survive the fabrication process and the 20+ years product warranty. At the busbar level, adhesion has been quantified using busbar pull-tests [1-4]; however, such a test is not readily applicable to testing the adhesion of metal fingers or to cells which are interconnected using strategies which do not require a busbar to be printed or plated on the cell [5-8]. Recently, a stylus-based adhesion tester was developed [9]. This approach, which is similar to the concept of a scratch test of

* Corresponding author. Tel.: +61-405-430-883.
E-mail address: ran.chen@student.unsw.edu.au

1876-6102 © 2015 The Authors. Published by Elsevier Ltd. This is an open access article under the CC BY-NC-ND license (http://creativecommons.org/licenses/by-nc-nd/4.0/).
Peer-review under the responsibility of Gunnar Schubert, Guy Beaucarne and Jaap Hoornstra
doi:10.1016/j.egypro.2015.02.087

thin films, allows quantitative measurements of adhesion characteristics on metal fingers. It was also used to map adhesion properties of plated metal fingers over the surface of a 156 mm solar cell.

In this paper, we report on the further development of the adhesion testing method introduced in [9] and apply the test to silver screen-printed fingers and nickel-copper plated fingers of laser doped selective emitter (LDSE) cells. The focus of this paper is on correlating the measured lateral force with the actual physical deformation of the fingers and thus identifying the observed failure modes. The uniformity of the measured results across a full wafer can reveal potential patterns of varying finger interfacial adhesion or finger bulk material properties, therefore identifying possible metallisation defects and enabling comparisons between different metallisation schemes and processing conditions.

2. Experimental

Two groups of cells were used in this study. Group 1 comprised industrially-produced 156 mm screen-printed cells with silver fingers of width ~ 100 μm. Group 2 comprised LDSE cells fabricated on 125 mm p-type, Cz-Si (100) wafers which were 180 μm thick with a full-area rear screen-printed and fired aluminium back surface field and electrode. The LDSE cells were phosphorus-diffused to a sheet resistance of ~ 80 Ω/ and then laser-doped with finger spacing of 1 mm before being plated using light-induced plating (LIP) of nickel and copper as described in [9].

The measurement probe of the adhesion tester was a customised high speed steel cylindrical stylus with a diameter of 0.7 mm (shown in Fig. 1). The top surface of the stylus was grinded to ensure flatness and then the stylus was mounted on a holder which was attached to a load cell. Two different load cells (Scaime AR0.2 and AR0.6) were used to provide a wider range of measurable force without sacrificing measurement accuracy. A signal amplifier and an A/D converter were used to sample the data from the load cell at variable frequencies. In this study, a frequency of 1000 Hz was used. The digital voltage signals received by the computer were converted to a time series of lateral force (in N) by using the calibration data from a digital force gauge (SunDoo SH-10).

The solar cell was mounted onto a customised ultra-flat (±10 μm) vacuum-enabled platen. Two parallel adhesive strips were applied on the cell surface spaced 2-3 mm apart and the stylus was placed at the centre of the spacing. The adhesive strips provide a constant boundary condition for finger dislodgement. During the measurement, the stylus was held still while the platen with the cell was moved at a constant speed of 0.5 or 1 mm/s. The translational direction of the platen was orthogonal to the orientation of the metal fingers.

Ten linear scans were performed for each cell. For each scan, a total of 70 and 120 fingers were deformed on the screen-printed and LDSE cells, respectively. The finger-to-finger spacing was 2.2 and 1.0 mm and the spacing between the scans was fixed as 15.6 and 10.5 mm for the screen-printed and LDSE cells, respectively. A high-magnification lens system was set up to monitor the dynamics of finger deformation and to reveal the failure modes.

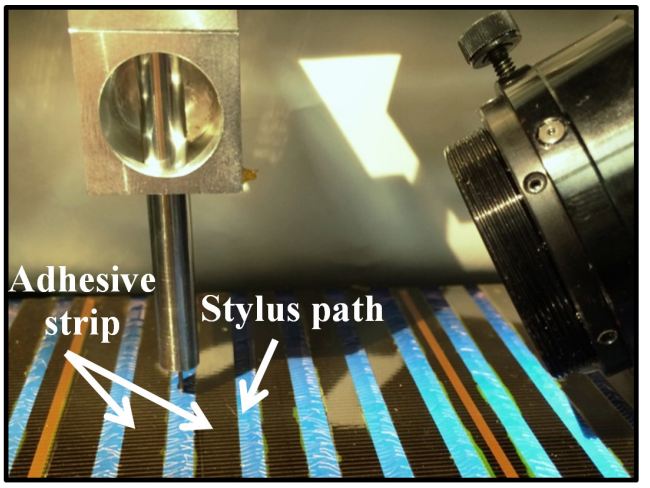

Fig. 1. Image of the adhesion tester showing the stylus moving across the cell dislodging fingers.

3. Results and discussion

The two distinct failure modes of: (i) finger cut-off; and (ii) dislodgement were identified from the video recordings and are shown in the captured images in Fig. 2. In cut-off mode (Fig. 2a), which was observed for the screen-printed silver fingers, the stylus cut through the silver finger. Metal residue typically remained on the cell surface at the cut-off region. The cutoff length was measured to be 0.7 mm which was the same as the diameter of the stylus. For the nickel/copper plated LDSE cells, fingers typically dislodged from the silicon with the dislodgement occuring for a distance wider than the diameter of the stylus as shown in Fig. 2b. Shortly after the dislodgement occurred, the dislodged finger broke at a position along the finger body leaving the stylus free to move unimpeded across the wafer surface again.

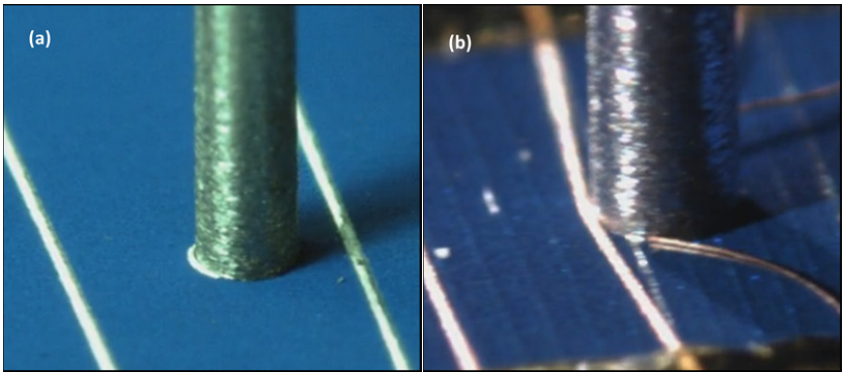

Fig. 2. In-situ images of the stylus tip: (a) cutting through a screen-printed silver finger; and (b) dislodging a nickel/copper plated finger on an LDSE cell. The diameter of the stylus was 0.7 mm. The finger-to-finger spacing was 2.2 and 1 mm for the screen-printed and plated fingers, respectively.

Fig. 3a schematically represents the recorded data when cut-off mode was observed and can be explained as follows. The substrate moves causing the surface to move relative to the stylus with a constant force being recorded until the stylus comes into contact with a finger at point A. While the substrate continues to move, a force is exerted

on the stylus leading to the bending of the load cell and an increasing force being recorded, which is represented by the section A-B in Fig. 3a. When the lateral force increases to ~ 4.5 N at point B, the finger cuts off almost instantaneously with a cut-off width of 0.7 mm. After it is released from the "loaded" position, the load cell is restored to its position initially overshooting, leading to a negative force at point C. Finally, the recorded force returns to its baseline value in preparation for measuring the next finger.

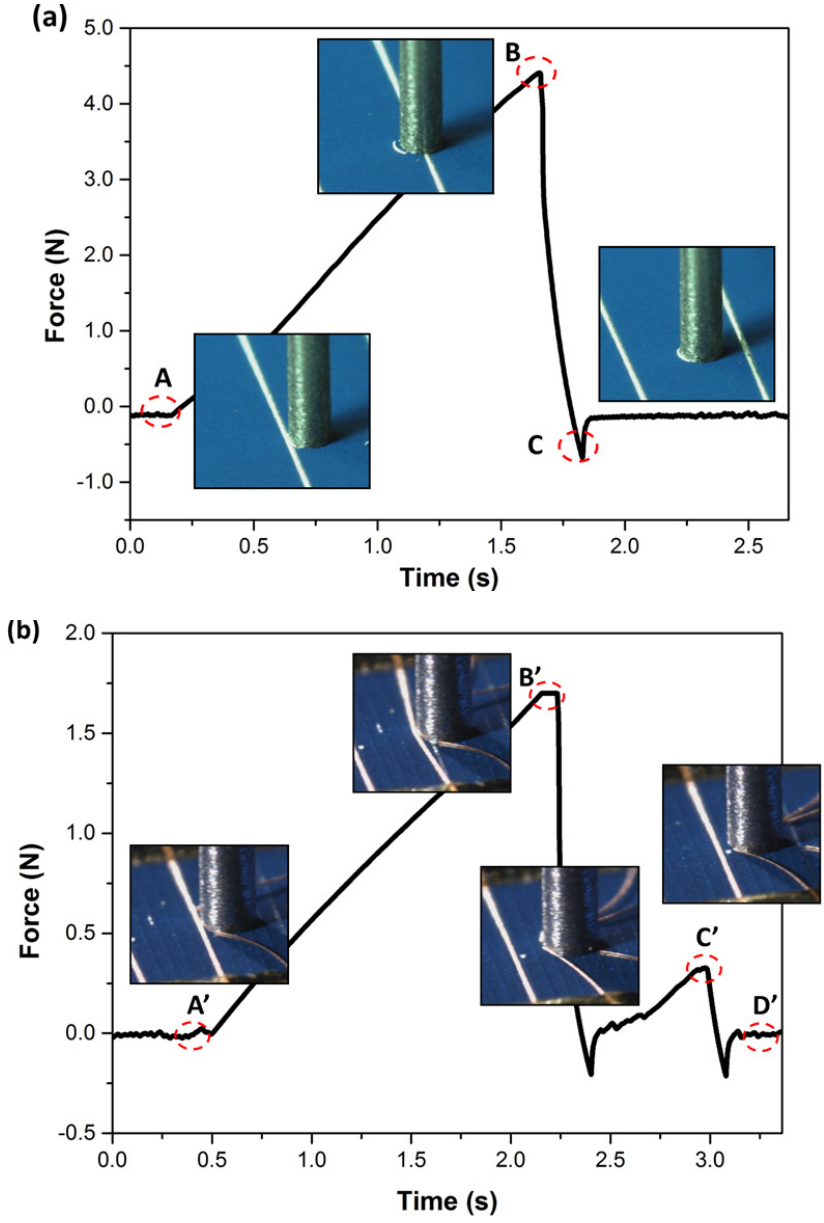

Fig. 3. Time series of lateral forces from testing one finger under: (a) cut-off mode; (b) dislodgement mode.

For the screen-printed fingers, most of the finger body in the cut-off section was removed by the stylus, leaving a residue of solid material at the cut-off region as shown in Fig. 4a. The force difference between points A and B was

interpreted as the cut-off force and the shear stress applied to the finger (in Pa) was estimated as the product of the measured cut-off area and the cut-off force. Although it is difficult to determine the shear strain from this measurement (which is required to estimate the shear modulus), the calculated shear stress can be used to compare the hardness of fingers resulting from the use of different silver pastes or different printing or firing processes [10]. For the screen-printed cells the cut-off force was used to construct a contour map for scanned cells.

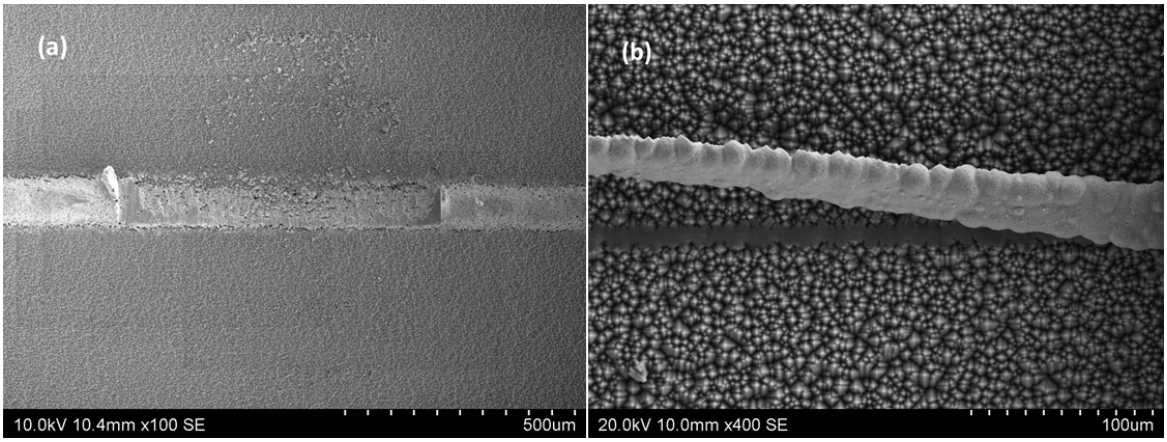

Fig. 4. SEM images of: (a) a cut-off region of a screen-printed finger; and (b) a dislodged region of a plated finger.

In dislodgement mode, as shown in Fig. 3b, the typical force curve arising from the dislodgement of a finger differed due to the different failure mode. The curve can be explained as follows. Point B' corresponds to the dislodgement of a finger from the silicon surface as shown in Fig. 4b. Due to the tensile strength of the finger, it does not break like the screen-printed finger but dislodges from the silicon a distance from the point of impact with the stylus. The extent or length of the dislodged finger can be, at most, the width of the region delineated by the adhesive tape (i.e., 2-3 mm). A second difference that is observed with this failure mode is the occurrence of a second peak, identified by point C' in Fig. 3b. This peak corresponds to when the dislodged finger breaks. The force difference between point A' and B' was recorded as the dislodgement force and used to construct the corresponding contour map. It represents a measure of the interfacial adhesion strength between the plated finger and the silicon wafer with higher forces being measured for more adherent fingers. However, the force difference between the baseline (i.e., points A' and D') and point C', i.e., breaking force, depends on the material properties of the plated finger (e.g., Young's modulus). However, the point C' does not consistently appear for each dislodged finger. It was observed that a higher dislodgement force, which corresponds to a larger bending of the load cell, leads to stronger restoring movement of the stylus. As a result, it appears that sometimes the finger breaks before the overshooting point of the stylus. Finally, after finger breaking, the stylus stabilises again at the baseline force at point D'. Young *et al.* proposed a so-called "peel length" test where the adhesive strip is not applied and the scan speed of the stylus is much faster (50 mm/s). The resulted peel length was assumed to be a metric of the finger tensile strength. In this study, since in-situ observations of the dislodging dynamics were achieved, the force difference between points C' and D' were considered a direct indication of finger tensile strength, or more specifically the Young's modulus of the plated metal. Further work will consider how this breaking force can be directly related to physical parameters of the metal fingers that can be directly measured by setting up a tensile strength tester specifically for plated contacts. However, even without this direct correlation, measurements of dislodgement force, peel distance and/or breaking force can be used to assess the benefits of changed processing (e.g., different line opening methods, different plating processes or chemistry).

It should be noted that cut-off and the dislodgement forces should not be directly compared as they arise from different failure mechanisms. For screen-printed fingers, the interfacial strength per unit area is typically stronger than the shear stress; however, for the plated nickel/copper fingers, the bulk strength of the fingers typically is much greater than the interfacial strength. These differences arise due to the metal bulk properties and also the geometry of the fingers. Screen-printing results in low aspect ratio fingers with a larger area that is beneficial for interfacial adhesion. Higher-aspect ratios can be achieved with plated metal fingers. Although this is beneficial from an optical perspective, it results in a reduced contact area and so it is critical that the interfacial adhesion is maximised for these contacts.

For both failure modes it is desirable to determine variability in contacting over the surface of the cell. The measured data acquired from a series of scans across a cell were used to construct contour maps of the wafer surface. To eliminate extraneous noise without removing the global trend, the data were smoothed before mapping. Along the scanning direction, every 10 cut-off forces and every 12 dislodgement forces were averaged for the screen-printed cell and the LDSE cells, respectively. The average values were used to construct the contour maps shown in Fig. 5.

Fig. 5a shows the results for the screen-printed cell, where the silver fingers were cut off with a mean cut-off force of 3.5 N and a standard deviation of 0.7 N. The variations in cut-off force appear to be random without any distinguishable patterns or trends across the cell. On the other hand, the contour map for the dislodgement force (mean of 0.62 N and standard deviation of 0.26 N) of plated LDSE cell, shown in Fig. 5b, exhibits a strong trend in dislodgement force. The fingers towards the end of scan #1 and #2 resulted a higher dislodgement force (i.e., 1-1.25 N) than the majority of the fingers which were dislodged at 0.5-0.75 N. And a valley of 0.25-0.5 N seems identifiable around the beginning fingers of scan #5 and #6. This trend may suggest the existence of non-uniformities introduced during the fabricating process of the plated LDSE cell that may have been caused by variations in the emitter doping profile, the way the laser-doping was performed or variations in the metal plating procedure.

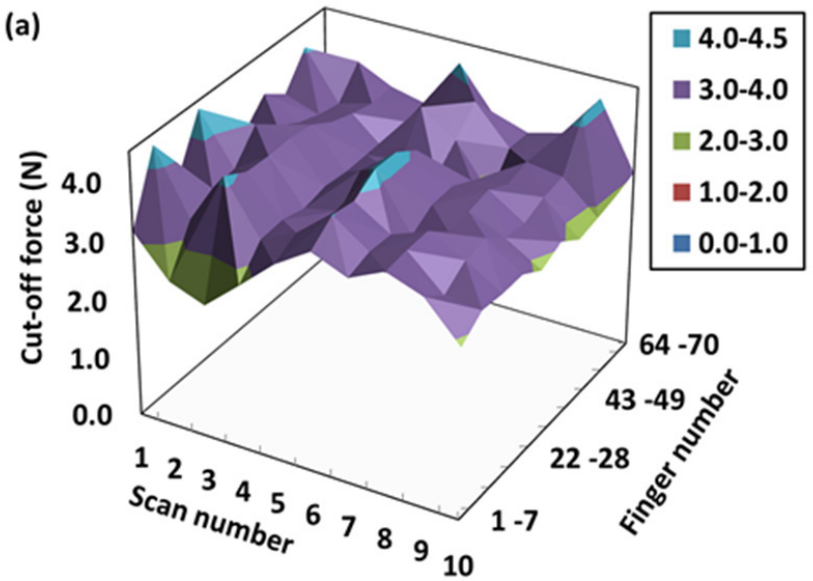

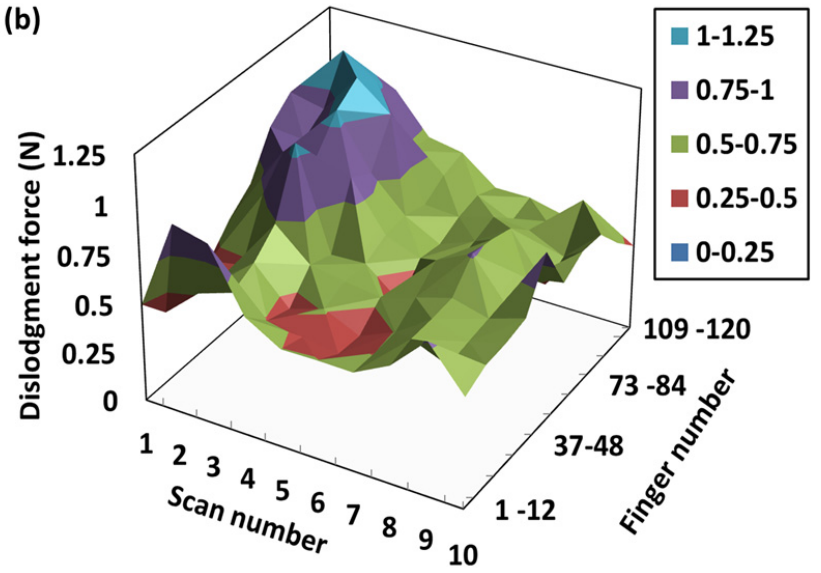

Fig. 5. Contour maps of cut-off force and dislodgment force for (a) screen-printed cell; (b) LDSE cell, respectively.

To also demonstrate the variation in adhesion properties across the cells, histograms of the non-averaged cut-off and dislodgement forces are shown in Fig. 6. The dislodgement force (Fig. 6b) has a significant positive tail which is largely caused by the higher plateau in the contour map (Fig. 5b). In contrast, the cut-off force (Fig. 6a) is much less skewed and 54.6% of the data is in the interval of 3-4 N. Thus, the contour map and the histogram can serve to identify the differences in the finger interfacial adhesion or the finger bulk material properties between different metallisation schemes and processing conditions.

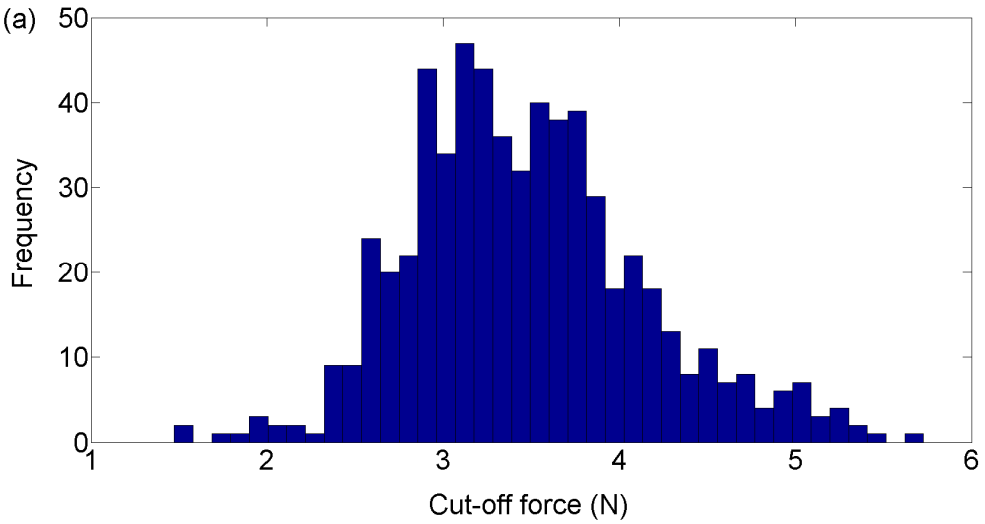

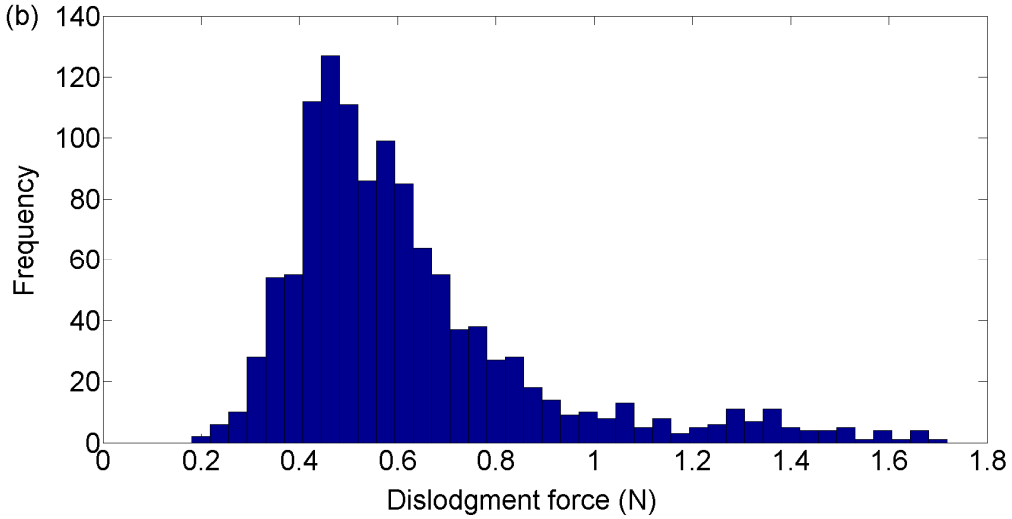

Fig. 6. Histogram of cut-off force and dislodgement force for: (a) a screen-printed cell; and (b) a LDSE cell.

4. Conclusion

A stylus-based adhesion tester was developed to quantify the adhesion properties of metal contacts with in-situ visualisation of failure modes across a silicon solar cell. Two distinct failure modes, finger cut-off and dislodgement, were identified and the measured forces associated with these failure modes were elucidated. Depending on the comparative contributions of interfacial adhesion and the material bulk properties, a particular failure mode dominates for different metallisation strategies. Contour maps of cut-off force and dislodgement force were used to demonstrate the uniformity of the corresponding adhesion properties of metal contacts across the surface of cells. For the screen-printed cell, no trend was identified; however, for the plated LDSE cell, significant trends in dislodgement force across the surface of the cell suggested the existence of process variation across the wafer.

References

[1] Jacobsson R, Measurement of the adhesion of thin films. Thin Solid Films, vol. 34, pp. 191-199, 1976.
[2] Wendt J, Trager M, Klengel R, Petzold M, Schade D, Sykes R, Improved quality test method for solder ribbon interconnects on silicon solar cells. Thermal and Thermomechanical Phenomena in Electronic Systems (ITherm), 2010 12th IEEE Intersociety Conference on, 2010. pp. 1-4.
[3] Mondon A, Jawaid MN, Bartsch J, Glatthaar M, Glunz SW. Microstructure analysis of the interface situation and adhesion of thermally formed nickel silicide for plated nickel–copper contacts on silicon solar cells. Solar Energy Materials and Solar Cells, vol. 117, pp. 209-213, 2013.
[4] Horzel J, Bay N, Passig M, Sieber M, Burschik J, Kühnlein H. Low cost metallisation based on Ni/Cu plating enabling high efficiency industrial solar cells. 29th European Photovoltaic Solar Energy Conference, Amsterdam, NL, 2014.
[5] Braun S, Hahn G, Nissler R, Pönisch C, Habermann D.The Multi-busbar Design: An Overview. Energy Procedia, vol. 43, pp. 86-92, 2013.
[6] Braun S, Nissler R, Ebert C, Habermann D, Hahn G. High Efficiency Multi-busbar Solar Cells and Modules. Photovoltaics, IEEE Journal of, vol. 4, pp. 148-153, 2014.

[7] Edwards M, Ji J, Sugianto A, Soederstroem T, Griscke R, Koschier L. High efficiency at module level with almost no cell metallisation: Multiple wire interconnection of reduced metal solar cells. 39th IEEE Photovoltaic Specialists Conference, Tampa, FL, 2013.

[8] Papet P, Söderström T, Ufheil J, Beyer S, Hausmann J, Meixenberger J. Front grid metallization and module interconnections of industrial heterojunction solar cells. 4th Workshop on Metallization for Crystalline Silicon Solar Cells, Constance, Germany, 2013.

[9] Young T, Hee K, Lennon A, Egan R, Wilkie O, Yao Y. Design and Characterization of an Adhesion Strength Tester for Evaluating Metal Contacts on Silicon Solar Cells. 40th IEEE Photovoltaic Specialists Conference Denver USA, 2014.

[10] Hannebauer H, Dullwerber T, Falcon T, Chen X, Brendel R. Record Low Ag Paste Consumption of 67.7 mg with Dual Print. Energy Procedia; 2013. 43(0): p. 66-71.